IEEE Access
Multidisciplinary | Rapid Review | Open Access Journal

Received 10 April 2025, accepted 21 May 2025, date of publication 26 May 2025, date of current version 2 June 2025.

Digital Object Identifier 10.1109/ACCESS.2025.3573590

RESEARCH ARTICLE

Design of Corrugated Horn Antenna for LEO Satellite Feeding System: Efficient Hybrid Optimization Approach

MAHMOUD GADELRAB[1] (Student Member, IEEE), SHOUKRY I. SHAMS[1] (Senior Member, IEEE), MAHMOUD ELSAADANY[2] (Senior Member, IEEE), AND GHYSLAIN GAGNON[2] (Senior Member, IEEE)

[1]Electrical and Computer Engineering Department, Concordia University, Montreal, QC H3G 1M8, Canada
[2]Département de Génie Èlectrique, École de Technologie Supèrieure, Montreal, QC H3C 1K3, Canada

Corresponding author: Mahmoud Gadelrab (Mahmoud.gadelrab@ieee.org)

ABSTRACT Low Earth Orbit (LEO) satellites are receiving fresh interest from the wireless communications society. The transceivers on these satellites require high-gain antennas with consistent performance over the operational spectrum. Corrugated horn antennas are the most typical feed used in such systems. Furthermore, several satellite systems use dual-polarized antennas to provide polarisation variety. However, simulating the full satellite feed transceiver is a time-consuming task. This paper presents a revolutionary hybrid technique that combines real-measured data with simulation tools to reduce the optimization time for the entire system while providing more accurate and robust results. This optimized design is fabricated using a CNC lathe machine with ± 0.002 inches accuracy. The fabricated prototype is measured in an anechoic chamber, where the measured results are in good agreement with the simulated ones.

INDEX TERMS Antenna evaluation, circular polarization, LEO feeding structure, system-level simulation, two-fold OMT.

I. INTRODUCTION

Demand for broadband satellite communications in the Ka-band is growing consistently, especially due to the higher data capacity required by different applications in the modern era. Giant corporations are competing to capture the market in satellite-based Internet services, as this is going to be one of the important sectors for Internet services in the future. In order to meet this demand, companies plan to deploy a constellation of small satellites in LEO orbit. A swarm of satellites is desired to support the enormous growth in related applications [1], [2]. The geostationary satellites are important due to their capability to use big multi-spot beam antennas and deliver considerable data throughput. However, the attractiveness of LEO satellites stems from their shorter round-trip time compared to Geostationary Orbit (GEO) satellites [3], [4]. Moreover, the position of LEO satellites offers several advantages such as lower losses, reduced round-trip delays, and the ability to utilize smaller satellites with lower power requirements [5], [6].

The feeding structure represents the main component of LEO satellite system design, where both signal transmission and reception are performed efficiently [7]. It consists of several elements that interact to provide signal transmission efficiently. In the framework of increasing system capacity, especially through frequency reuse, Circularly Polarized (CP) systems are especially useful because they reduce the multipath effects in wireless channels quite drastically compared with linearly polarized antennas of similar radiation characteristics [8], [9]. Besides, polarization diversity can be obtained by using Orthomode Transducers (OMTs) that can transmit or receive CP waves of different rotational senses simultaneously [10], [11], [12], [13]. The correct prediction of the system response is crucial for design,

The associate editor coordinating the review of this manuscript and approving it for publication was Tutku Karacolak.

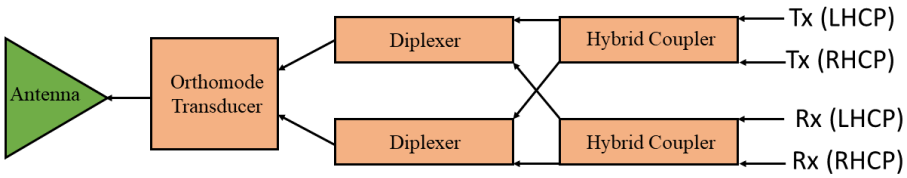

FIGURE 1. Block diagram for the Ka-feeder system indicating the measured components of the system (Couplers, Diplexer, and OMT), and the simulated component (corrugated horn antenna).

optimization, and cost reduction, which are very relevant problems when dealing with high-frequency components of challenging fabrication associated with high cost and long time frame.

The antenna in such systems is among the most complicated and costly parts, particularly when dealing with corrugated horn designs. Corrugated horns are preferred as feed structures for reflector antennas due to two primary factors. Firstly, they possess a symmetric radiation pattern, enabling the construction of high-gain antennas with minimal spillover. Secondly, these horns exhibit exceptionally low levels of cross-polarization, a crucial requirement in dual-polarization systems. The key feature of corrugated horn antennas lies in their unique structure, which includes periodic corrugations along the inner walls of the waveguide. These corrugations are crucial in controlling the electromagnetic field distribution and improving the antenna's performance [14], [15], [16], [17].

The corrugated horn antennas are fabrication cost and tolerance-sensitive, particularly when dealing with Ka-band design [18], [19]. Simulation packages solve real-world problems safely and efficiently, as it provides an important method of analysis that is easily verified and understood. However, this approach often requires significant computational resources and may necessitate multiple iterations of fabrication and testing, particularly for the antenna. This process is not appropriate in terms of system-level simulation for microwave components and antenna structure. This demand for first-pass design success requires an accurate predictive model to be available for the subsystem components of the whole system, enabling the antenna design to be simulated and optimized with a real-time signal. This will save time and the cost of unnecessary fabrication and testing of the corrugated horn antenna.

This paper proposes a novel methodology that incorporates actual measurements with simulation tools to predict the overall system response without the need to simulate the entire system. By fabricating and testing some components, and then feeding these measured results into the simulation environment, we aim to achieve an accurate representation of the system's performance, particularly the antenna response, thereby reducing the need for multiple fabrications.

II. SYSTEM DESCRIPTION & SPECIFICATIONS

Circularly polarized systems are widely used in communication systems like satellite telecommunication, offering advantages over linear polarizations and requiring precise alignment between transmitter and receiver terminals. The electromagnetic spectrum can be more efficiently utilized by using two orthogonal signals (RHCP and LHCP), increasing link capacity. Each polarization can be used for transmitting or receiving, or even simultaneously, with frequency discrimination achieved through diplexers [20], [21]. LEO satellite feeders widely use signals with single or dual orthogonal circular polarizations [22]. The proposed design used here in this paper is shown in the block diagram Fig.1.

TABLE 1. System specifications.

Frequency-Tx (lower band)	17..7-20.2 GHz
Frequency-Rx (Higher band)	27.5-30 GHz
VSWR	1.25:1
Axial Ratio	0.5 dB
RHCP/LHCP Isolation	17 dB
Tx/Rx Isolation	80 dB

This system consists of 4 main components, the first one is the orthomode transducer (OMT) which functions as a separator of the orthogonal linearly polarized signals. The second one is the diplexers which separate the frequency into the Tx/Rx bands. The last one is the hybrid couplers that produce the 90° phase shift between the signals. The most commonly used antenna in this structure is the corrugated horn type. This type of antenna possesses a symmetric radiation pattern, enabling the construction of high-gain antennas with minimal spillover [23], [24].

The generic Ka-band frequency and polarisation plan are shown in the table 1, indicating the overall system specification. The system is a six-port network electrically, and five-port physically. The intended matching level on both ports is around 20 dB. The isolation between the left-handed and right-handed ports for both cases is around 17 dB. The other key design targets are an axial ratio (AR), of 0.5dB or better. Moreover, the used diplexers are expected to provide around 80 dB rejection between Tx/Rx bands. This feeder is designed to feed a Cassegrain reflector system, therefore some radiation characteristics of the antenna should be taken into consideration, which are highlighted in the next section.

III. FEED SYSTEM CORRUGATED HORN ANTENNA

The corrugated horn antenna is pivotal in advanced communication systems, recognized for its superior radiation pattern, low cross-polarization levels, and broad bandwidth capabilities. In antenna design, the challenge lies in optimizing these performance parameters while addressing practical implementation issues. For standard applications,

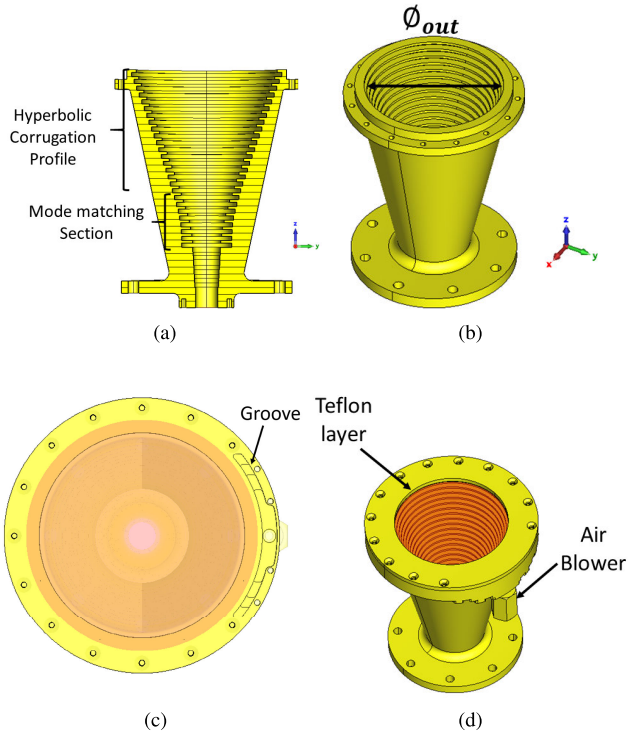

FIGURE 2. The proposed corrugated horn design indicates, (a) the corrugations' cross-sectional view, (b) a 3D structure with an outer diameter (ϕ_{out}), (c) groove for the air blower, and (d) a face cover with an air blower system.

the propagating mode in the horn is the HE11 mode, which produces a radiation pattern close to a Gaussian shape. Maintaining this Gaussian-pattern characteristic over the operating bandwidth is crucial to meeting cross-polarization, return-loss, and sidelobe requirements. Typically, a corrugated horn connects to a circular, smooth-walled input waveguide, where the fundamental mode is TE11. This necessitates a mode converter to transition smoothly from the TE11 mode to the HE11.

It is worth mentioning that the TM11 mode will be excited by the main mode TE11 as it passes through the different depth slots due to discontinuity. However, the phases of the E- and H-planes are not consistent, which will affect the system's overall performance. The phase relationship between the E- and H-planes is crucial for achieving the desired axial ratio, making phase consistency a key factor in the system's efficiency [25].

A. ANTENNA SPECIFICATIONS

1) MECHANICAL

The antenna requires a cover on its face and an air blow system for several important reasons, primarily related to maintaining performance and protecting the antenna structure. An air blower hose is employed to direct airflow through a dedicated groove in the antenna's aluminum cover. The cover is sealed with silicone to maintain a pressurized environment, ensuring it can effectively withstand the incoming air pressure. The cover, often made from a material that is transparent to the operational electromagnetic frequencies, protects the antenna's delicate internal corrugations from environmental elements such as dust, moisture, and debris. These contaminants can degrade the performance by altering the designed electromagnetic properties of the horn.

2) ELECTRICAL

The proposed antenna should overcome the previously mentioned problems. Hence, the required gain for the antenna should be around 23 dBi. A symmetric 1 dB variation should be maintained between the E-plane and H-plane patterns of the antenna. Furthermore, the edge tapering should be around 19 dB making it suitable for Cassegrian or Gregorian reflector systems. Finally, all these radiation characteristics should not be affected when adding the cover material.

B. PROPOSED DESIGN

This design is categorized as a wideband application, covering a frequency range from 17.7 GHz to 30 GHz. This wide bandwidth requires additional critical requirements on the antenna design. The input diameter ϕ_{in} of the antenna is chosen to ensure the propagation of the dominant TE11 mode while avoiding the excitation of higher-order modes. In this case, the input diameter is chosen to be $\phi_{in} = 0.45$inch followed by a circular waveguide transition as shown in Fig. 2 (a). For the mode conversion section, a variable-depth slot mode converter is used, typically comprising five to seven slots. The choice of the corrugation profile is another vital consideration that affects the radiation pattern characteristics of the antenna. Several types of corrugation profiles are commonly used, including linear, sinusoidal, and exponential profiles. Recently, the Gaussian profile has gained popularity due to its superior performance, and the hyperbolic profile, which is equivalent to the Gaussian profile, is also frequently utilized. The main body of the corrugated horn is then constructed using a hyperbolic profile with a variable number of slots as shown in Fig 2 (b). This overall design is modeled using CST Microwave Studio Macros to ease the optimization of changing the number of corrugations in mode conversion and horn body simultaneously [26]. Finally, a Teflon layer is chosen as a cover to the antenna as shown in Fig. 2 (c).

IV. SIGNALS EXCITATION

As highlighted in the previous system architecture, simulating the entire system is a time-consuming process, particularly while terminating with radiating elements. The antenna design in this system is critical, especially in meeting the axial ratio specification below 0.5 dB. Achieving this axial ratio requires precise control of both the phase and amplitude between the right-hand and left-hand circularly polarized signals. Even slight manufacturing tolerances can impact these parameters, challenging ensuring compliance with the desired axial ratio. Instead of optimizing the entire system, which would demand significant computational resources, this project proposes a more efficient approach by

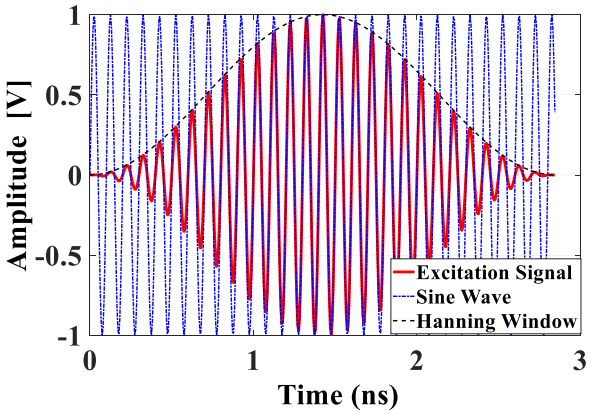

FIGURE 3. Time domain representation for the default CST excitation signal.

feeding the antenna with real measurement signals from the fabricated components. We will perform the simulation and the antenna optimization using CST Microwave Studio fed by the actual measured response. This method significantly reduces the time and computational burden while ensuring that the antenna meets the performance requirements, especially regarding the axial ratio, without full numerical system optimization.

A. MATHEMATICAL FORMULATION OF PROPOSED EXCITATION

In Microwave Studio CST, the excitation signals are key elements in electromagnetic systems' time domain simulation process. These are the driving forces of the simulation, exciting the model with energy in the form of electromagnetic waves that enable analysis of the system's behavior under various conditions. Proper selection and setting of excitation signals are significant prerequisites for achieving accurate simulations at antenna design or other microwave structures. The primary excitation signal employed in CST is a sine wave modulated by a Hanning window, as described in detail in the simulation package manual [26]. This signal is depicted in Fig. 3, which is mathematically expressed as:

$$S(t) = \sin(2\pi ft) \times \frac{1}{2}(1 - \cos(2\pi n/N)) \tag{1}$$

such that, f represents the center frequency, and the signal length is defined as $L = N + 1$. The sampling index of the signal is n and its condition is $0 \leq n \leq N$.

1) MEASURED DATA

The satellite feeder components in Fig. 1 are assembled to extract the excitation signal to feed the antenna. The system evaluation is done in two stages. The first stage is the matching level measurement using a circular load termination as shown in Fig. 4 (a). The achieved return loss value for both bands is around 20 dB which is indicated in Fig. 4 (b) and (c). In the second stage, we measure the transmitted signal and predict the axial ratio without the antenna contribution. This stage is more challenging as an extra OMT is used as shown

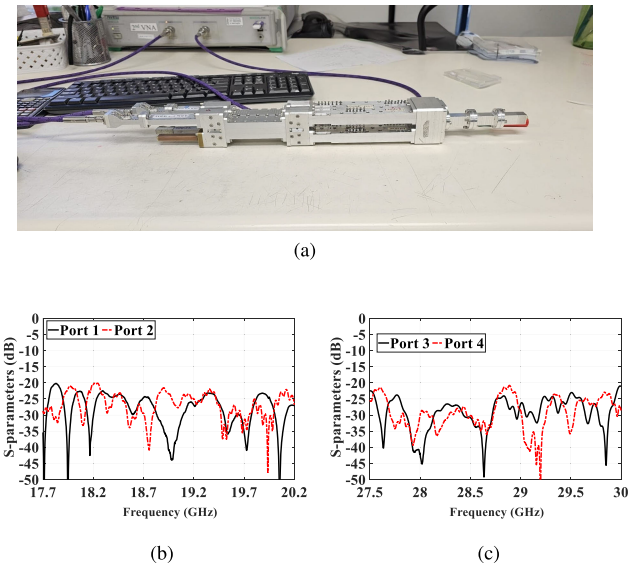

FIGURE 4. Return loss measurement for the Ka-feeder, (a) measured setup with a circular load termination, (b) lower band response. (c) higher band response.

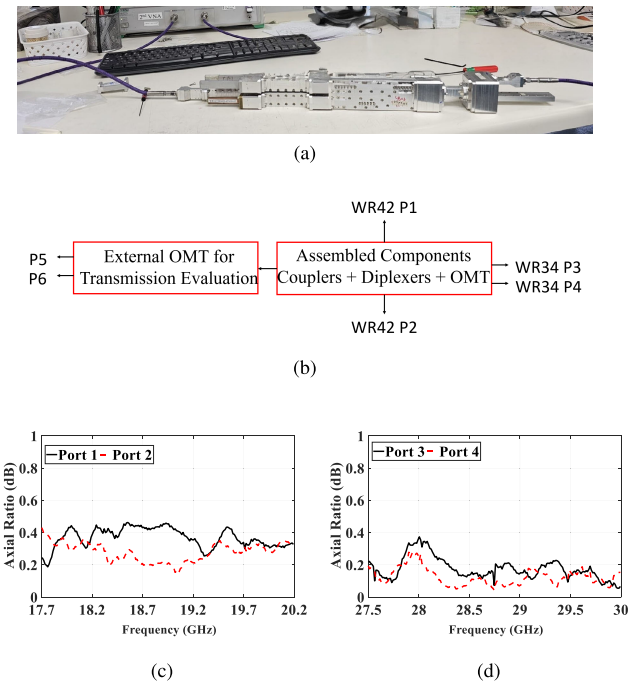

FIGURE 5. Axial ratio for the Ka-satellite feeding system without the antenna, (a) block diagram for the system, (b) the lower band calculated axial ratio, and (c) the higher band calculated axial ratio.

in Fig. 5 (a). This results in a 6-port network as in the block diagram in Fig. 5 (b), then the following equation can be used to calculate its value [9],

$$A = \sqrt{\frac{|S_{51}|^2 + |S_{61}|^2 + |S_{56}|^2}{|S_{51}|^2 + |S_{61}|^2 - |S_{56}|^2}} \tag{2}$$

$$S_{56} = \sqrt{|S_{51}|^4 + |S_{61}|^2 + 2|S_{51}|^2|S_{61}|^2 \cos(2\phi_{56})} \tag{3}$$

such that, S_{51} and S_{61} are the transmissions from the coupler port 1 to the virtual two ports of the OMT, while the $\phi_{56} = \angle S_{51} - \angle S_{61}$ represents the phase difference between both polarizations. This results in curves shown in Fig. 5 (c) and (d) with a value near the 0.5 dB for both bands.

2) SIGNAL FORMULATION

The transmitted signal measured from the fabricated system is illustrated in Fig. 6 (a). These signals denoted as $M(\omega)$, are in the frequency domain where the lower band corresponds to the Tx signals, and the higher band represents the Rx signals. This signal is composed of the real and imaginary parts of the as shown in Fig. 6 (b). However, these signals are in the frequency domain, they cannot be directly used as excitation signals in CST. To use the measured signals as excitation inputs in CST, the first step is to transform the CST default signal 1 into the frequency domain using a Fourier transform, as follows:

$$S(\omega) = \int_{-\infty}^{\infty} S(t)e^{-j\omega t}, dt \tag{4}$$

Afterwards, the measured signal is multiplied by the CST excitation signal in the frequency domain:

$$E(\omega) = S(\omega)M(\omega) \tag{5}$$

Finally, applying an inverse Fourier transform to the resulting signal yields the time-domain signal:

$$E(t) = \frac{1}{2\pi}\int_{-\infty}^{\infty} E(\omega)e^{j\omega t}, dt \tag{6}$$

which results in the signal shown in Fig. 7. This signal is fed into the CST Microwave Studio as an input signal. This will guarantee a good estimation of the simulation of the corrugated horn antenna and how the antenna with different tolerances will affect the predicted results.

B. OPTIMIZED ANTENNA DESIGN

The proposed antenna design mentioned previously in Fig. 2 is modeled in CST using equations to draw the profiled corrugations. The mode conversion section is chosen to be a variable-depth-slot mode converter where the number of slots N_{mc} varies between five to seven slots. The slot depth of the j th slot is calculated using the following equation

$$d_j = \left(\sigma - \frac{j-1}{N_{Mc}}\left(\sigma - \frac{1}{4}\exp\left[\frac{1}{2.114(k_o a_j)^{1.134}}\right]\right)\right)\lambda_o \tag{7}$$

where $0.4 \leq \sigma \leq 0.5$ is the percentage factor for the first slot depth of the mode converter, and k_o and λ_o are the center frequency wave number and its corresponding wavelength respectively. The initial value for this frequency is around $1.2\, f_{min}$ which is around 21 GHz. The profiled corrugation follows a hyperbolic profile as follows [23],

$$\phi(z) = \sqrt{\phi_{in}^2 + \frac{z^2(\phi_o^2 - \phi_{in}^2)}{L}} \tag{8}$$

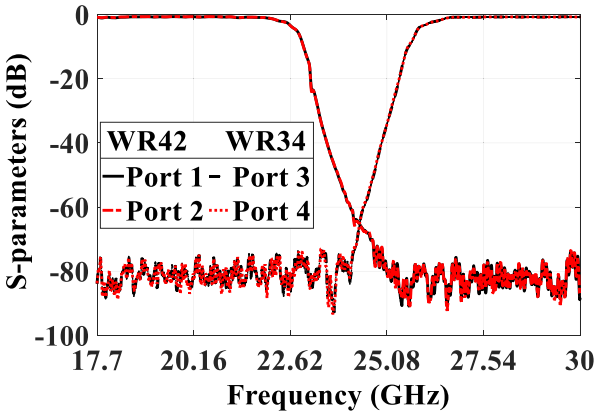

(a)

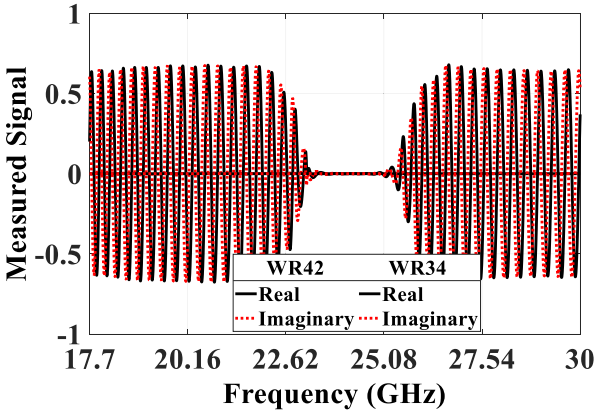

(b)

FIGURE 6. Transmitted signal from the satellite system, (a) insertion loss for both frequency bands, and (b) real & imaginary parts of the signal.

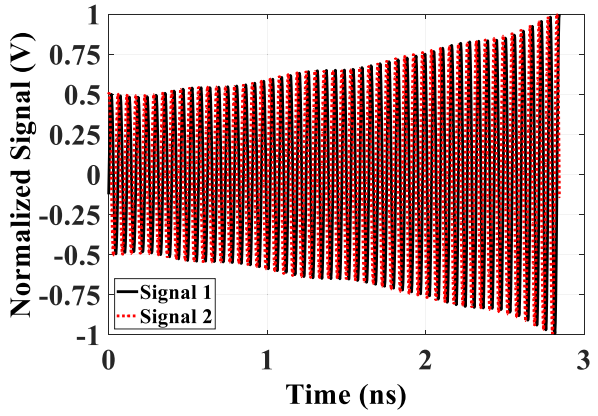

FIGURE 7. Feed signals results from the inverse Fourier transform and imported into CST corrugated horn file.

where ϕ_{in} and ϕ_o are the input and output circular waveguide diameters respectively. While the total length of the antenna is referred to as L. A circular waveguide transition is used in the input interface to match between the input circular waveguide diameter $\phi_{in} = 11.43$ mm and the corrugated section as shown in Fig. 8. Afterward, this antenna is simulated using the excitation signal shown in Fig.7, and the design is

TABLE 2. The optimized values for the circular waveguide transitions.

Parameter	Value (mm)	Parameter	Value (mm)	Parameter	Value (mm)
ϕ_1	12.3	ϕ_7	13.8	l_4	2.4
ϕ_2	12.6	ϕ_8	14.1	l_5	2.2
ϕ_3	12.9	ϕ_9	14.4	l_6	3.1
ϕ_4	13.1	l_1	2.2	l_7	2.1
ϕ_5	13.4	l_2	2.3	l_8	1.8
ϕ_6	13.7	l_3	2.1	l_9	2.54

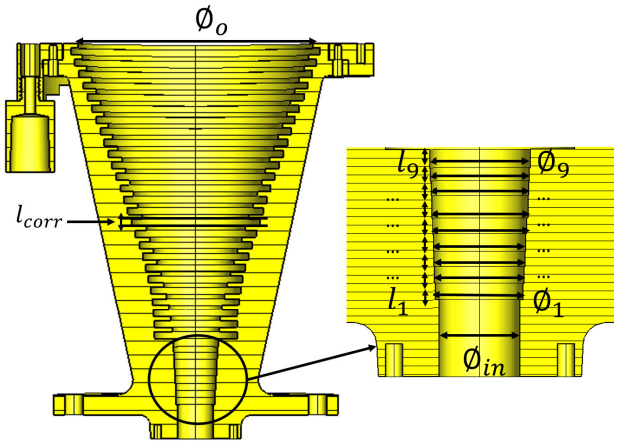

FIGURE 8. Final optimized parameters for the corrugated horn antenna.

optimized to achieve a matching level below 25 dB. Another optimization goal is the symmetrical radiation pattern in the E & H plane with a deviation below 1 dB difference within the suspended angle. Finally, the axial ratio goal is below 0.5 dB for both bands of the feeding system. The mode converter section ends up with 5 slots and the corrugation pitch length is $l_{corr} = 2.1336$ mm. While the overall length of the antenna is 123.825 mm that corresponds to 25 slots with an outer diameter of the antenna is $\phi_o = 81.25$ mm. The optimized dimensions for circular waveguide transition are in table 2.

V. ANTENNA MEASUREMENTS & VALIDATION

The fabrication process of a corrugated horn antenna involves several meticulous steps to ensure high precision and performance. Computer Numerical Control (CNC) lathe machines are used to realize the inner surface horn corrugations accurately. Once the primary structure is completed, the horn undergoes surface chemical treatment processes to avoid oxidization and enhance its durability. The fabricated unit is shown in Fig. 9 where the Teflon and the air blower section are added to the antenna. The overall system is assembled with the antenna to perform the experimental evaluation.

A. MEASUREMENT SETUP

The return loss for the antenna is measured using a waveguide calibration for both bands and the achieved results are shown in Fig. 10 (a) and (b) where it achieves around 20 dB for both bands. The gain of this antenna exceeds 15 dB, as mentioned earlier, making the planar near-field scanner

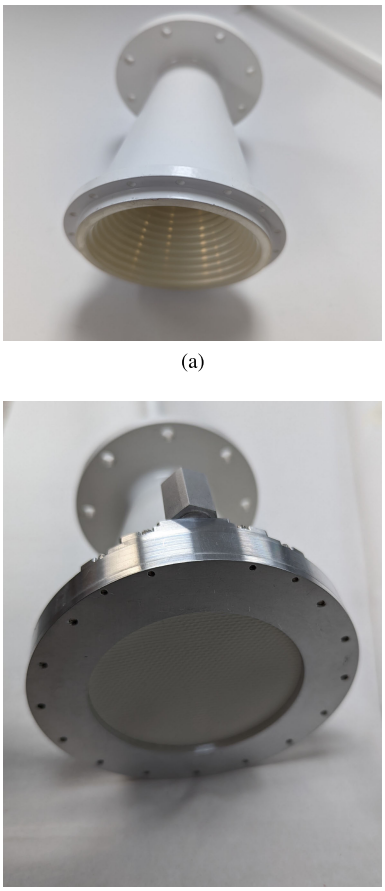

(a)

(b)

FIGURE 9. The fabricated corrugated horn design (a) the unit without the antenna seal, and (b) the unit with the face cover and the air blower.

highly suitable for its testing [27], [28], as depicted in Figure 10 (a). Being a dual-band antenna, the measurements were conducted using two open-ended waveguide probes. The WR42 probe measures the lower frequency band (17.7-20.2 GHz), while the WR28 probe captures the higher frequency band (27.5-30 GHz). Both probes were rotated between 0 and 90 degrees during the measurements to obtain dual-polarized data. Accordingly, four measurements are carried out. Afterward, a transformation from Near Field to Far Field (NF-FF) transformation is carried out using NSI-software [29]

B. RADIATION PATTERNS

Four separate measurements were conducted for the four-port feed system depicted in Fig. 1. The results from these

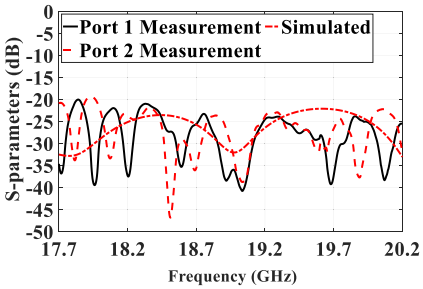

(a)

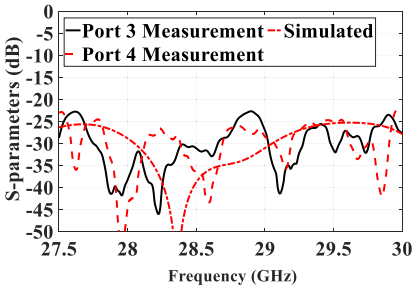

(b)

(c)

FIGURE 10. Satellite feeding measurements, (a) the lower band measured return loss (b) the higher band measured return loss, and (c) the anechoic chamber measurements for the radiation pattern.

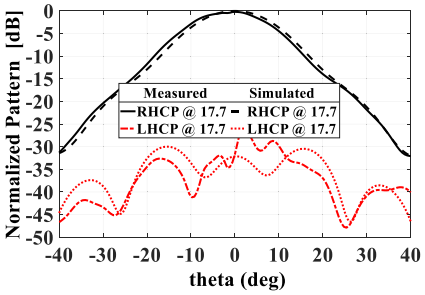

(a)

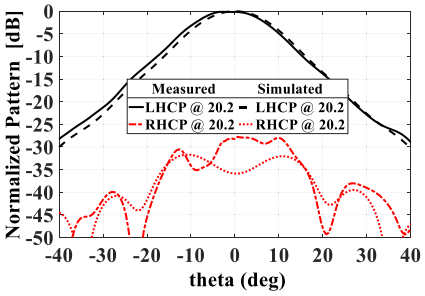

(b)

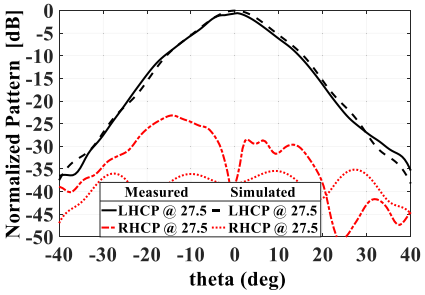

(c)

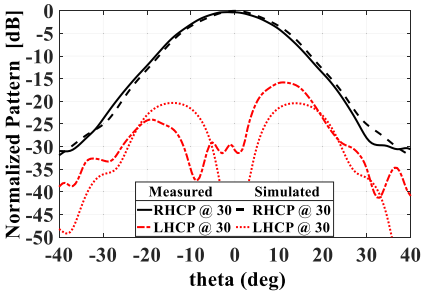

(d)

FIGURE 11. Radiation pattern measurements versus simulations (a) RHCP (port 1) at 17.7 GHz, (b) LHCP (port 2) at 20.2 GHz, (c) LHCP (port 3) at 27.5 GHz, (d) RHCP (port 4) at 30 GHz.

measurements demonstrate excellent agreement with the simulation data, as highlighted in Fig. 11. The E- and H-plane radiation patterns are nearly identical, exhibiting an edge taper of approximately 19 dB. This close alignment between the patterns confirms the antenna's balanced performance across both planes. Furthermore, the measured gain of the antenna was compared to the simulated gain, as illustrated in Fig. 12 (a) and (b). The comparison shows the antenna flat gain response and a good agreement with the simulations.

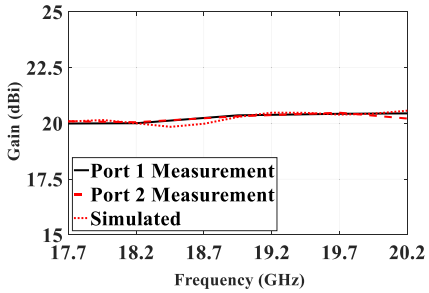

(a)

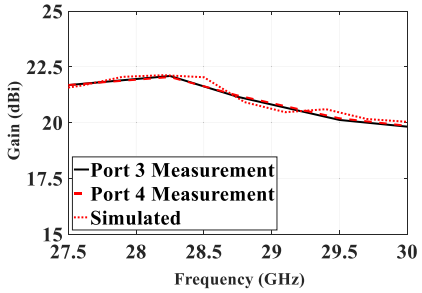

(b)

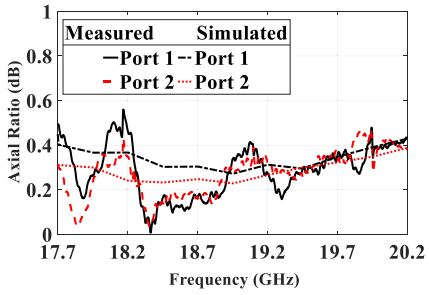

(c)

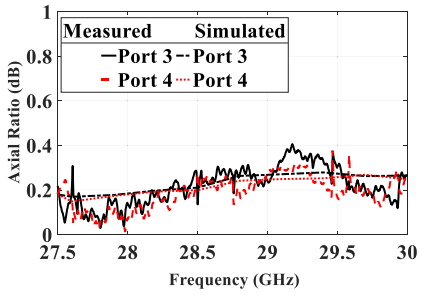

(d)

FIGURE 12. Antenna experimental evaluation (a) lower band gain (b) higher band gain (c) lower band axial ratio (d) higher band axial ratio.

Moreover, the axial ratio (AR) was computed from the cross-polarization (XP) values using the following equation [30]:

$$AR|_{dB} = 20\log\left(\frac{1+10^{\frac{XP}{20}}}{1-10^{\frac{XP}{20}}}\right) \tag{9}$$

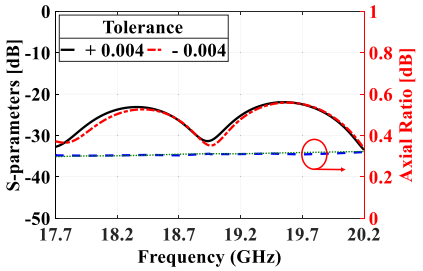

(a)

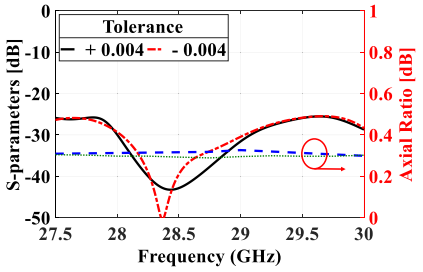

(b)

FIGURE 13. Tolerance analysis for the system on (a) lower band, and (b) higher band gain.

The calculated axial ratio for the four ports is presented in Fig. 12 (c) and (d), demonstrating that the antenna radiates a circularly polarized wave. These measured AR values are in close agreement with the simulation, further confirming the accuracy and effectiveness of the antenna system design. This indicates the antenna's suitability for applications requiring dual-polarization and high gain.

C. TOLERANCE ANALYSIS

Analyzing tolerance is important in this scenario as even slight mechanical or alignment mistakes in polarizing elements can cause considerable impairment in antenna functionality, especially regarding axial ratio and cross-polarization levels. By measuring the horn's resilience to such changes, the tolerance analysis provides essential insights into the feasibility of the design and guarantees that it remains effective despite real-world variations in fabrication and assembly. This enhances the design's suitability for high-reliability applications like satellite communication systems. Thus, the tolerance for the proposed design is discussed for adding a sensitivity of about ± 0.004 inches to see its effect on the overall system. The results obtained from this analysis is shown in Fig. 13, where the results for the return loss is affected by 0.5 dB for both bands. Moreover, the axial ratio is not affected that much. However, the level of the axial ratio in the higher band is changed by around 0.1 dB.

D. PROPOSED DESIGN PERFORMANCE EVALUATION

To assess the performance of the proposed antenna system, a comparison with previous designs is presented in Table 3. The proposed antenna is compared with other

TABLE 3. Comparison of performance.

Ref.	Freq (GHz)	Gain (dBi)	XPL (dB)	Isolation (dB)
[31]	45-90	-	-18.8 -14.4	-
[32]	18.3-20.2 28.3-30	> 16	-	70
[33]	19.6-21.2 29.5-31	-	-30 -27	-
[34]	8-18 32-40	> 14.3 > 20.1	-17.5 -19	81 72
This Work	17.7-20.2 27.5-30	> 19.5 > 20	-25 -15	80 -80

antenna systems either circular polarized [31], [33], [34] or Linear polarized [32]. The proposed antenna operates effectively across dual frequency bands: 17.7-20.2 GHz and 27.5-30 GHz, covering typical Ka-band allocations for LEO satellite communication systems. Other antennas covers different dual bands, and achieves a gain of around 16 to 20 dBi [32], [34]. However, the proposed antenna achieves a gain exceeding 19.5 dBi for both bands of operation. In terms of the cross polarization level, the proposed design achieves −25 dB in the lower band in the beamwidth of (−40 to 40) degrees. However, the higher band achieves −15 in the same beamwidth. For full duplex systems [32], [34], it can achieve an isolation level of about 70 to 80 dB. In the proposed design, it achieves 80 dB isolation clear for both bands.

VI. CONCLUSION

This paper introduces a novel technique for the design optimization of corrugated horn antennas in large complicated systems. By combining a real-measured system with simulation tools, this technique enables the prediction of overall system reaction without the need to simulate the whole system. The antenna's overall performance with the system was measured in an anechoic chamber. The obtained results using this technique agree with the simulation response, highlighting a high accuracy level for this approach.

REFERENCES

[1] L. You, K.-X. Li, J. Wang, X. Gao, X.-G. Xia, and B. Ottersten, "Massive MIMO transmission for LEO satellite communications," *IEEE J. Sel. Areas Commun.*, vol. 38, no. 8, pp. 1851–1865, Aug. 2020.

[2] Y. Du, S. Liu, Z. Fang, and S. Gao, "Reliability evaluation of all-user terminals in LEO satellite communication network based on modular reduction," *China Commun.*, vol. 19, no. 2, pp. 235–246, Feb. 2022.

[3] T. Goel, S. Pelluri, and A. Patnaik, "A CRLH-SIW based frequency-reconfigurable antenna for LEO to GEO inter-satellite link," in *Proc. IEEE Indian Conf. Antennas Propogation (InCAP)*, Dec. 2018, pp. 1–5.

[4] B. R. Elbert, *Introduction to Satellite Communication* (Artech House Space Applications Series). Norwood, MA, USA: Artech House, 2008. [Online]. Available: https://books.google.com.eg/books?id=_vqOgUwtWfIC

[5] M. Yang, X. Dong, and M. Hu, "Design and simulation for hybrid LEO communication and navigation constellation," in *Proc. IEEE Chin. Guid., Navigat. Control Conf. (CGNCC)*, Aug. 2016, pp. 1665–1669.

[6] J. Lin, Z. Hou, Y. Zhou, L. Tian, and J. Shi, "Map estimation based on Doppler characterization in broadband and mobile LEO satellite communications," in *Proc. IEEE 83rd Veh. Technol. Conf. (VTC Spring)*, May 2016, pp. 1–5.

[7] R. Roberts, P. Booth, G. Fox, S. Stirland, and M. Simeoni, "Q/V-band feed system development," in *Proc. 10th Eur. Conf. Antennas Propag. (EuCAP)*, Apr. 2016, pp. 1–5.

[8] F. A. Dicandia, S. Genovesi, and A. Monorchio, "Analysis of the performance enhancement of MIMO systems employing circular polarization," *IEEE Trans. Antennas Propag.*, vol. 65, no. 9, pp. 4824–4835, Sep. 2017.

[9] S. Shams, A. M. Mahfouz, M. Elsaadany, M. A. M. Hassan, G. Gagnon, and A. A. Kishk, "Circularly polarized V-Band orthomode transducer," *IEEE Antennas Wireless Propag. Lett.*, vol. 22, no. 1, pp. 29–33, Jan. 2023.

[10] M. Gadelrab, S. I. Shams, and A. Sebak, "Compact dual linear polarized antenna feed for LEO satellites based on quad ridge waveguide," in *Proc. Int. Telecommun. Conf. (ITC-Egypt)*, Jul. 2023, pp. 210–214.

[11] M. Gadelrab, S. I. Shams, and A. R. Sebak, "Dual linear polarized antenna feed for LEO satellites," in *Proc. Int. Telecommun. Conf. (ITC-Egypt)*, Jul. 2022, pp. 1–4.

[12] M. Gadelrab, "LEO satellite feeding system: Design and analysis," Ph.D. dissertation, Dept. Elect. Comput. Eng. (ECE), Concordia Univ., Montreal, QC, Canada, 2023.

[13] M. A. AbdElraheem, M. Gadelrab, S. I. Shams, and A. Sebak, "Compact double ridged asymmetric orthomode transducer for low Earth orbit satellite applications," in *Proc. Int. Telecommun. Conf. (ITC-Egypt)*, Egypt, Jul. 2024, pp. 217–220.

[14] P. J. B. Clarricoats and P. K. Saha, "Propagation and radiation behaviour of corrugated feeds. Part 2: Corrugated-conical-horn feed," *Proc. Inst. Electr. Eng.*, vol. 118, no. 9, p. 1177, 1971.

[15] C. Dragone, "Reflection, transmission, and mode conversion in a corrugated feed," *Bell Syst. Tech. J.*, vol. 56, no. 6, pp. 835–867, Jul. 1977.

[16] G. G. Gentili, E. Martini, R. Nesti, and G. Pelosi, "Performance analysis of dual profile corrugated circular waveguide horns for radioastronomy applications," *IEE Proc.-Microw., Antennas Propag.*, vol. 148, no. 2, p. 119, Apr. 2001.

[17] M. Gadelrab, S. I. Shams, and A. R. Sebak, "An ultra wide band quad horn antenna with different ridges profiles," in *Proc. IEEE Int. Symp. Antennas Propag. USNC-URSI Radio Sci. Meeting (AP-S/URSI)*, Jul. 2022, pp. 1802–1803.

[18] A. Gonzalez, K. Kaneko, and S. Asayama, "Recent work on (Sub-)mm-Wave ultra wideband corrugated horns for radio astronomy," in *Proc. 11th Eur. Conf. Antennas Propag. (EUCAP)*, Mar. 2017, pp. 3327–3331.

[19] J. Teniente, J. C. Iriarte, I. Ederra, and R. Gonzalo, "Advanced feeds for mm-Wave antenna systems," *Aperture Antennas Millim. Sub-Millim. Wave Appl.*, vol. 2017, pp. 75–110, Sep. 2017.

[20] Y. Yu, B. Liu, Y. Wang, and Q. S. Cheng, "Automated diplexer design with key performance indicator-based objectives," *IEEE Microw. Wireless Compon. Lett.*, vol. 32, no. 7, pp. 827–830, Jul. 2022.

[21] H. Khalil, Syed-ur-Rehman, and D. M. Minhas, "Comparison of S band diplexer design using multiplexer theory with coupling matrix synthesis," in *Proc. Int. Symp. Technol. Manage. Emerg. Technol. (ISTMET)*, Aug. 2015, pp. 243–248.

[22] P. Kohl, M. Kilian, M. Schneider, and C. Hartwanger, "A compact dual band polariser for Q/V-band," in *Proc. 14th German Microw. Conf. (GeMiC)*, May 2022, pp. 9–12.

[23] C. Granet and G. L. James, "Design of corrugated horns: A primer," *IEEE Antennas Propag. Mag.*, vol. 47, no. 2, pp. 76–84, Apr. 2005.

[24] P.-S. Kildal, *Foundations of Antenna Engineering: A Unified Approach for Line-of-sight and Multipath*. Norwood, MA, USA: Artech House, 2015.

[25] H. Wang, Z. Lu, Y. Liu, J. Yu, Y. Yao, X. Liu, and X. Chen, "Design of a tanh profiled compact Gaussian corrugated horn for Cassegrain antenna application," in *Proc. Asia acific Microw. Conf. (APMC)*, vol. 2, Dec. 2015, pp. 1–3.

[26] *CST Microwave Studio*, CST Studio Suite, Dassault Systèmes Simulia, Vélizy-Villacoublay, France, 2023.

[27] A. C. Newell, "Error analysis techniques for planar near-field measurements," *IEEE Trans. Antennas Propag.*, vol. 36, no. 6, pp. 754–768, Jun. 1988.

[28] G. Hindman, S. Gregson, and A. Newell, "Accurate Planar Near-FieldResults Without Full Anechoic Chamber," in *Proc. 36th Annu. Meetingand Symp. Antenna Meas. Techn. Assoc. (AMTA)*, Nov. 2014, pp. 1–6.

[29] *NSI2000 Standard Edition Software*. [Online]. Available: https://www.nsi-mi.com/products/software-products/nsi2000/2000-standard-edition

[30] C. A. Balanis, *Antenna Theory: Analysis and Design*. Hoboken, NJ, USA: Wiley, 2016.

[31] K. K. Chan and S. K. Rao, "Design of high efficiency circular horn feeds for multibeam reflector applications," *IEEE Trans. Antennas Propag.*, vol. 56, no. 1, pp. 253–258, Jan. 2008.

[32] S. Manafi, M. A. Al-Tarifi, and D. S. Filipovic, "Isolation improvement techniques for wideband millimeter-wave repeaters," *IEEE Antennas Wireless Propag. Lett.*, vol. 17, pp. 355–358, 2018.
[33] J.-R. Qi, Y. Dang, P.-Y. Zhang, H.-T. Chou, and H.-S. Ju, "Dual-band circular-polarization horn antenna with completely inhomogeneous corrugations," *IEEE Antennas Wireless Propag. Lett.*, vol. 19, no. 5, pp. 751–755, Mar. 2020.
[34] Y. Tao, C. Deng, X. Cao, and K. Sarabandi, "A full-duplex dual wideband horn antenna with high port-to-port isolation," *IEEE Trans. Antennas Propag.*, vol. 72, no. 11, pp. 8876–8881, Nov. 2024.

MAHMOUD GADELRAB (Student Member, IEEE) received the B.Sc. degree in communications engineering from German University in Cairo (GUC), in 2021, and the Master of Applied Science degree from Concordia University, in 2023. His research interests include ferrite-based structures, ridge gap waveguide technologies, and satellite feeding structures. He received GUC Top Ranking Students Scholarship, in 2016, and maintained this award, until 2021. He was awarded the Concordia Supervisor's Research Grant.

SHOUKRY I. SHAMS (Senior Member, IEEE) received the B.Sc. (Hons.) and M.Sc. degrees in electronics and communications engineering from Cairo University, Cairo, Egypt, in 2004 and 2009, respectively, and the Ph.D. degree in electrical and computer engineering from Concordia University, Montreal, QC, Canada, in 2016. From 2005 to 2006, he was a Teaching and Research Assistant with the Department of Electronics and Communications Engineering, Cairo University. From 2006 to 2012, he was a Teaching and Research Assistant with the Institute of Engineering and Technology (IET) Department, German University in Cairo. From 2012 to 2016, he was a Teaching and Research Assistant with Concordia University. His research interests include microwave reciprocal/nonreciprocal design and analysis, high-power microwave subsystems, antenna design, and material measurement. He received the Faculty Certificate of Honor, in 1999, and the Distinction with Honor, in 2004, from Cairo University. He was a recipient of the Concordia University Recruitment Award, in 2012, and the Concordia University Accelerator Award, in 2016. He was German University in Cairo (GUC)-IEEE Student Branch Chair, from 2010 to 2012.

MAHMOUD ELSAADANY (Senior Member, IEEE) received the B.Sc. (Hons.) and M.Sc. degrees in electrical engineering from Cairo University, Giza, Egypt, in 2006 and 2010, respectively, and the Ph.D. degree in electrical and computer engineering from Concordia University, Montreal, QC, Canada, in 2018. He is currently an Assistant Professor with the ECE Department, Concordia University, and also a Research Professional with École de Technologie Supérieure (ETS), Université du Québec, Montreal. He was a Researcher with Qatar University, Doha, Qatar, from 2008 to 2010. His current research interests include digital signal processing, optimization of microwave components, machine-type communication, and algorithm design for 5G cellular networks.

GHYSLAIN GAGNON (Senior Member, IEEE) received the Ph.D. degree in electrical engineering from Carleton University, Ottawa, ON, Canada, in 2008. He is currently a Full Professor and the Dean of Research with the École de Technologie Supérieure, Université du Québec, Montréal, QC, Canada. His research interests include CMOS IC design, digital signal processing, and machine learning with various applications. He was also the Director of LACIME Research Laboratory, from 2013 to 2020, a group of 15 professors and 150 highly dedicated students and researchers in microelectronics, digital signal processing, and wireless communications. He is highly inclined toward collaborative research with industry and was awarded the 2020 Partnership and Innovation Award from ADRIQ.